

## Lectures

---

### THE STRUCTURE AND PROPERTIES OF PLASMA SPRAYED ALUMINA COATINGS\*

R. McPHERSON

*CSIRO Division of Materials Science and Technology  
Clayton, 3168, Victoria, Australia*

#### 1. INTRODUCTION

Alumina, in sintered form, is the most widely used of the so-called advanced ceramics and is also the most commonly used thermally sprayed ceramic coating because of its excellent wear resistance, refractory and electrical properties at relatively low cost. The earliest commercial alumina coatings were produced by the "Rokide" process, in which the tip of a sintered rod was melted by means of an oxygen acetylene torch and the resulting molten droplets projected onto a suitable substrate, or by injecting powder into a combustion flame [1]. Later developments involved injection of powders into a high velocity combustion pulse jet (detonation gun) [2], or direct current plasma jet [3]. The common feature of these processes is the formation of a stream of molten particles, the major differences between them the particle size and velocity.

More recently low pressure plasma spraying (LPPS) has been employed for the application of dense metallic coatings, particularly oxidation resistant coatings for gas turbine blades and reactive metals such as titanium and tantalum [4]. The use of a low pressure, inert environment allows the preparation of a clean substrate surface, elimination of oxide contamination of metallic coatings and high velocity jet conditions. The use of a low pressure environment does however introduce problems with heat and momentum transfer to particles in the spray stream [5]. The LPPS process has had limited application to ceramic coating but there is evidence that higher density coatings can be achieved by this means [6].

Early studies of the structure of thermally sprayed coatings revealed that they had an unusual microstructure, consisting of a collection of rapidly solidified lamellae, which obviously gave them properties quite different to conventionally processed materials. The present paper examines the relationship between the structure and properties of alumina coatings with particular reference to those produced by plasma spraying.

#### 2. THE SPRAYING PROCESS

The plasma jet consists of a high velocity, high temperature stream of gas in which there are large spatial temperature and velocity gradients. Particles must be introduced into the jet in such a way that they completely melt and accelerate

---

\*Paper read at the 5th Conference on Aluminium Oxide, Prague, 27—30 August 1990

to a high velocity, in the short residence time available, if high density coatings are to be achieved [7]. The feed particles must be small enough to melt completely but not so small that vaporisation becomes significant; in practice this means a particle size range between about 10 and 100  $\mu\text{m}$ . The powder must have good flow properties so that it can be efficiently injected into the plasma jet and the particles should be in a physical form which favours rapid melting. Mono-sized particles prepared by fusion provide these characteristics and lead to high quality coatings [8]. The powder injection parameters are important because they strongly influence the path taken by particles through the plasma jet; at low injection velocities particles may not penetrate the high temperature core, at high injection velocities they may pass transversely through it. There is thus a significant technology associated with the design of the torch system and powder characteristics to reliably achieve high quality coatings [9].

### 3. THE COATING FORMATION PROCESS

Coatings are formed by the successive impact of molten droplets which rapidly spread over the substrate, or previously solidified material, and each solidifies to form a disc-shaped lamella. As will be shown, this lamellar microstructure dominates the properties of thermally sprayed coatings. A simplification of an analysis of the impact of molten droplets, originally due to Madjeski [10], based on the assumption that the spreading and solidification processes could be treated separately [7, 11], gave the following relationship:

$$\xi = 1.29(\rho d v / \eta)^{0.2},$$

where  $\xi$  is the ratio of the flattened disc diameter  $D$  to the drop diameter  $d$ ,  $\rho$  is the drop density,  $v$  the drop velocity and  $\eta$  the drop viscosity.

This is in good agreement with observation; the lamellar thickness of conventionally plasma-sprayed alumina coatings is about 3  $\mu\text{m}$  [12]. Solidification of such thin lamellae is similar to splat quenching and other rapid solidification processes in which the cooling rate is of the order of  $10^6 \text{ K s}^{-1}$ .

Since each lamella solidifies independently onto much cooler material there is a large constrained thermal contraction between the crystallisation temperature and ambient temperature, particularly for refractory materials like alumina, which gives rise to thermal stresses that considerably exceed the fracture stress and the lamellae therefore microcrack [13].

A further important conclusion arising from consideration of the droplet impact process is that adsorbed or entrapped gas under spreading droplets gives rise to imperfect contact between the solidified lamellae [13].

The formation process therefore leads to the major microstructural features of plasma sprayed ceramic coatings, namely, overlapping, randomly deposited, microcracked, rapidly solidified lamellae a few micrometres thick between which there is imperfect contact.

### 4. THE CRYSTALLINE STRUCTURE OF ALUMINA COATINGS

A feature of the structure of thermally sprayed alumina coatings, which surprised early workers, was that they consisted not of  $\alpha\text{-Al}_2\text{O}_3$ , the only stable form of alumina, but a metastable defect spinel structure, usually referred to as  $\gamma\text{-Al}_2\text{O}_3$ .

in the thermal spraying literature, which until then had been regarded as a low temperature form [14]. The  $\alpha$ - $\text{Al}_2\text{O}_3$  structure is trigonal with  $\text{Al}^{+++}$  occupying octahedral sites whereas  $\gamma$ - $\text{Al}_2\text{O}_3$  is based on face centred cubic packing of  $\text{O}^{--}$  with  $\text{Al}^{+++}$  occupying both octahedral and tetrahedral sites. The formation of the spinel based structure in coatings is clearly related to the rapid cooling rate from the melt inherent in the spraying process and it has been suggested that it could be related to „quenching in” of the presumed coordination of  $\text{Al}^{+++}$  in the liquid state [15].

A more satisfactory explanation may be provided by the classical nucleation theory which takes into account the relative nucleation of alternative crystalline forms from the undercooled melt [16]. The energy barrier to homogeneous nucleation is related to the driving force for the process (the free energy difference between the liquid and crystalline phases) and the interfacial energy between the liquid and the crystalline embryo. Thus  $\gamma$ - $\text{Al}_2\text{O}_3$  nucleates from undercooled melts in preference to  $\alpha$ - $\text{Al}_2\text{O}_3$  because it has an interfacial energy with liquid sufficiently low to compensate for its lower driving force. If the cooling rate is sufficiently high to prevent the transformation of  $\gamma$ -to  $\alpha$ - $\text{Al}_2\text{O}_3$ , then the former is retained to ambient temperature. The temperature-time relationship during cooling, which is influenced by the release of the heat of fusion, depends upon the lamellar thickness. Estimates

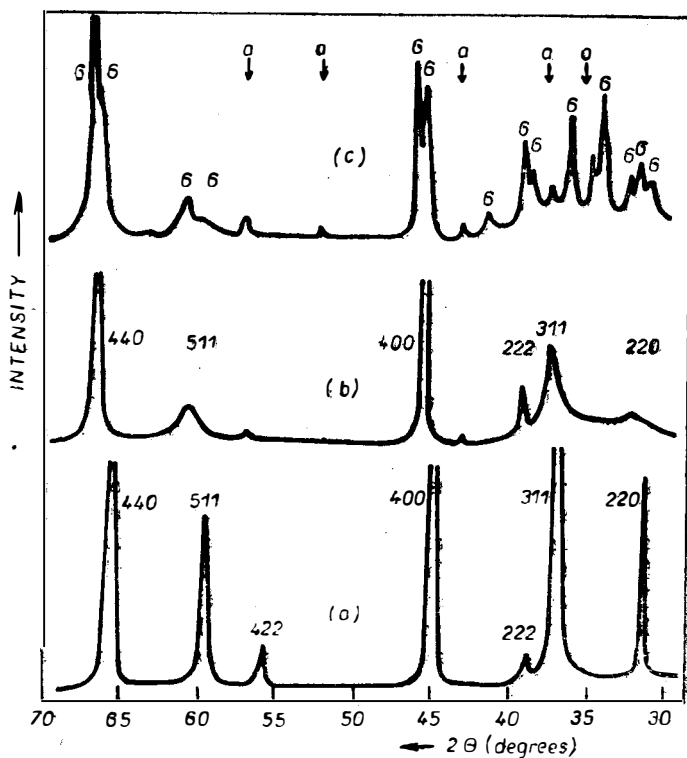


Fig. 1. X-ray diffraction patterns of plasma sprayed coatings: (a) spinel,  $\text{MgAl}_2\text{O}_4$ ; (b) alumina; and (c) alumina after heating for 4 hours at  $1000^\circ\text{C}$ .

of the thermal history in conjunction with the transformation kinetics suggest that lamellae thicker than about 20  $\mu\text{m}$  would consist of  $\alpha\text{-Al}_2\text{O}_3$  [11] and this is observed in occasional thick lamellae within coatings arising from large droplets accidentally formed on the powder feed inlet. Alpha alumina is also observed for similar reasons in coatings prepared by high frequency plasma spraying which employs large particle size powder and low impact velocity [17].

Plasma sprayed alumina coatings commonly contain some  $\alpha\text{-Al}_2\text{O}_3$  which arises from the incorporation of incompletely melted droplets, an effect which can be readily seen by optical transmission microscopy of thin sections under crossed polars because  $\gamma\text{-Al}_2\text{O}_3$  is optically isotropic whereas  $\alpha\text{-Al}_2\text{O}_3$  is birefringent [13]. This suggests a means for the preparation of  $\alpha\text{-Al}_2\text{O}_3$  coatings; if each of the powder particles contained at least one small particle of a material with higher melting point than alumina which did not dissolve in it during spraying, it could act as a heterogeneous nucleus, reducing the undercooling to favour nucleation of the alpha phase.

The X-ray diffraction patterns (Fig. 1) of plasma sprayed alumina and spinel ( $\text{MgAl}_2\text{O}_4$ ) show that the spinel based alumina peaks vary considerably in width and the (422) peak is missing. The (220) peak, for example, has a half height width of about  $2^\circ 2\theta$  whereas (222) is only  $0.3^\circ$  wide. Examination of the structure factors for the spinel structure shows that the (220) and (422) peaks arise only from the cations in tetrahedral sites, the sharpest peak, (222), from the oxygen lattice and octahedrally coordinated cations. The other peaks which have intermediate widths, have contributions from both tetrahedral and octahedral cations. The X-ray diffraction pattern of plasma sprayed alumina therefore suggests that it has the cubic spinel structure but that there is some sort of substructure associated with the distribution of  $\text{Al}^{+++}$  and vacancies in the tetrahedral sites.

Transmission electron microscopy has revealed that coatings do indeed have a complex substructure which may be interpreted as quasiperiodic antiphase boundaries of type  $(h00) a_0/4[011]$  between small ordered domains [18, 19]. This structure is associated with the high cation vacancy of 2.66 per unit cell required for the spinel structure of alumina. Heat treatment of coatings in the temperature range 500 to 800°C leads to anomalous changes in elastic modulus but negligible change in the X-ray diffraction pattern [20]. X-ray diffraction of alumina coatings heat treated to 1000°C for several hours clearly shows transformation to the ordered,  $\delta\text{-Al}_2\text{O}_3$  structure (Fig. 1) in which cationic vacancies are located at antiphase boundaries [21]. The presence of  $\delta\text{-Al}_2\text{O}_3$  can be readily detected by splitting of the (400) peak and this is sometimes observed in coatings which have been heated by the torch during spraying. Thus there seems to be a range of metastable structures possible in plasma sprayed alumina coatings, depending upon the temperature reached during spraying, which are based on the spinel structure, but have various arrangements of the cations associated with differing, more or less complex, domain substructures. The  $\gamma$ -type structures observed in coatings are apparently different in detail from the  $\gamma$ - and  $\eta\text{-Al}_2\text{O}_3$  forms derived from boehmite and bayerite which inherit structural features from the original mineral and which may also contain residual hydroxyl ions [22].

Heat treatment at approximately 1200°C results in transformation of the metastable, as-sprayed structure, to  $\alpha\text{-Al}_2\text{O}_3$  which is accompanied by an increase in porosity [23] because its density ( $4.0 \text{ gm cm}^{-3}$ ) is higher than that of  $\gamma\text{-Al}_2\text{O}_3$  ( $3.6 \text{ gm cm}^{-3}$ ). Heating to higher temperatures results in shrinkage as the porosity [23] is reduced by sintering [20]. Attempts have been made to prepare  $\alpha\text{-Al}_2\text{O}_3$

coatings by spraying on to heated substrates, however, a substrate temperature of about 1400 °C is required to obtain a dense deposit [24].

Coatings prepared from Al<sub>2</sub>O<sub>3</sub> based alloy powders may show interesting effects. Solutions of TiO<sub>2</sub> and Y<sub>2</sub>O<sub>3</sub> in  $\gamma$ -Al<sub>2</sub>O<sub>3</sub>, for example, are formed at concentrations which exceed their equilibrium concentrations in  $\alpha$ -Al<sub>2</sub>O<sub>3</sub> and the excess is precipitated on heat treatment [25] whereas coatings containing approximately 50 wt % Cr<sub>2</sub>O<sub>3</sub> form an  $\alpha$ -phase solid solution [26]; Al<sub>2</sub>O<sub>3</sub> — 34 to 64 wt % ZrO<sub>2</sub> coatings are amorphous [27].

Crystallisation of the lamellae making up a coating is nucleated at the surface in contact with previously solidified material and proceeds by rapid crystal growth into the undercooled liquid. The lamellae therefore have a microstructure which consists of columnar grains, approximately 0.2  $\mu$ m in diameter, which extend completely through them [28].

## 5. THE PORE STRUCTURE OF COATINGS

As pointed out above, it has been postulated that interlamellar contact within plasma sprayed ceramic coatings is imperfect, because of entrapped gas under impinging droplets, implying the presence of narrow pores within which there are regions of real contact [13]. Transmission electron microscopy of transverse sections of alumina coatings provided direct evidence of this and revealed the presence of pores about 0.1  $\mu$ m wide between lamellae within which there were regions of contact equivalent to grain boundaries [28]. In addition to these pores there were microcracks, around 0.1  $\mu$ m wide, within lamellae arising from thermal stresses. Mercury intrusion porosimetry of alumina coatings has also shown that a pore size of about 0.1  $\mu$ m is significant implying that the connecting channels between larger pores are of this size [29].

The real area of contact between lamellae, based on published elastic modulus measurements, was estimated to be approximately 25 % of the apparent area [13]. Recently, the morphology of the pores within alumina coatings has been directly delineated by scanning electron microscopy of transverse sections of samples in which the open porosity was filled with copper by an electroplating technique [12]. Quantitative analysis of the images [30] gave values for the true area of contact between lamellae of 20 to 30 %, in good agreement with previous estimates [13].

The proportion of true contact between lamellae could be expected to be related to the spraying process, for example, to the particle impact velocity in atmospheric spraying. Evidence for this is provided from published elastic modulus data which suggests that the interlamellar contact increases in the order flame, plasma, detonation gun [31]. Low pressure plasma spraying would also be expected to lead to improved interlamellar contact [13].

## 6. MECHANICAL PROPERTIES OF COATINGS

The mechanical properties of coatings are of considerable practical importance for most of their applications. It is well known that the mechanical strength of ceramic coatings is relatively low, as is their adhesive strength to metallic substrates. On the other hand, they exhibit a remarkable ability to withstand large

permanent deformation and severe thermal stresses without failure [14]. The unusual behaviour of ceramic coatings compared with their sintered counterparts is clearly related to microstructure.

### 6.1 Elastic Modulus

Measurements by Ault [14] of the Young's modulus of alumina coatings by a sonic resonance technique gave values of 34 to 40 GPa. Tucker compared the modulus of coatings prepared by plasma spraying and the detonation gun process and reported values of 39 and 94 GPa respectively. Fargeot et al. [32] reported 31 GPa for the Young's modulus of plasma sprayed alumina coatings, determined by resonance measurements at ambient temperature. Modulus measurements of alumina coatings at elevated temperatures, using a velocity of sound method, showed substantial changes which could be related to phase change and sintering effects [20]. Measurements by deflection of beams cut from alumina coatings gave values for the modulus at low strain in the range 20 to 50 GPa for flame sprayed and 60 to 90 GPa for plasma sprayed material; the stress strain curves obtained were non-linear [33].

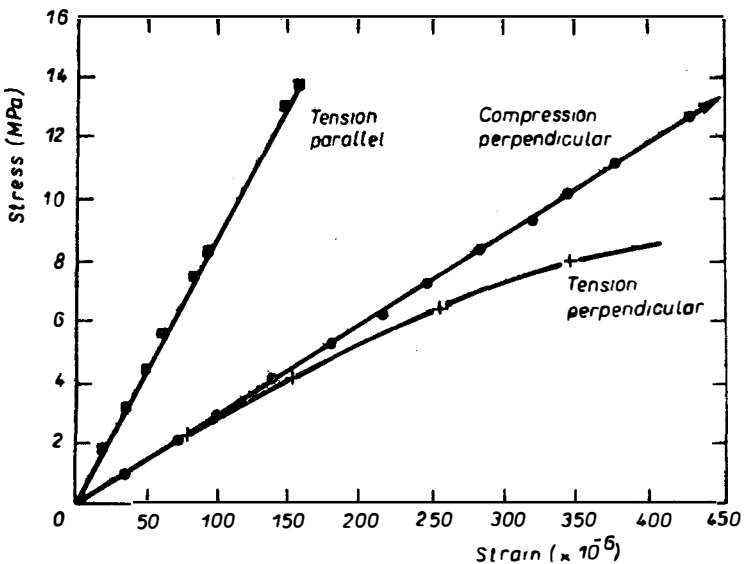


Fig. 2. Stress strain curves for a plasma sprayed alumina coating measured in tension and compression perpendicular to the coating plane and in tension parallel.

Recently, measurements of the apparent Young's modulus of plasma sprayed alumina coating perpendicular and parallel to the coating plane, from stress-strain curves determined using small strain gauges, gave values of 29 GPa perpendicular to the coating plane and 88 GPa parallel to it [31]. The stress strain curves were linear elastic in compression perpendicular to the coating plane and in tension parallel to it, but non linear elastic in tension perpendicular to the coating plane.

The Young's modulus of dense sintered  $\alpha$ - $\text{Al}_2\text{O}_3$  is about 400 GPa and is reduced to approximately 300 GPa at 10 % porosity [34]. The very low values observed for coatings can be partly explained by a lower modulus for the metastable form, however, a major part of the difference must be associated with the microstructure as observed, for example, in Ni coatings in which the modulus may be 15 to 40 % of the value observed for the dense material depending on pore volume and morphology [35]. A simple view is that the modulus is directly related to the effective real contact area between lamellae [13] and this approach provides a satisfactory model for the modulus of Ni-Al coatings, which have a simple microstructure, but not for Ni coatings with a more complex structure [35].

The elastic anisotropy and non linear elastic response of plasma sprayed alumina coatings perpendicular to the coating plane have been explained as follows [30]. The low modulus perpendicular to the coating plane is proportional to the mean real area of contact between lamellae at low strain, but at higher strains the thin interlamellar pores, which are clamped together by residual stress, open to provide an additional component to the total strain. The process reverses on unloading giving non linear elastic behaviour. The structure parallel to the coating plane may be regarded as similar to a jig-saw puzzle consisting of interlocking pieces, arising from the microcracked lamellae, and the modulus is related to frictional effects between the pieces and shear deformation of the true contact regions.

## 6.2 Fracture Toughness

An understanding of the fracture behaviour of ceramics requires knowledge of a material parameter related to the resistance to crack initiation or propagation. In the case of coatings two parameters are of interest, one associated with fracture at the interface with the substrate, that is, for adhesive failure, and another related to fracture within the coating, that is, for cohesive failure. It has been shown that it is possible to determine such parameters for alumina coatings by means of the double cantilever beam (DCB) technique in which a coated steel bar has a similar bar attached to it by an adhesive, and a crack is propagated either through the coating, or along the coating-substrate interface by applying a tensile opening force at the end of the beam [36]. Values of the critical strain energy release rate ( $G_{Ic}$ ), which may be regarded as the energy per unit area required to propagate the crack, were in the range 10 to 15  $\text{Jm}^{-2}$  for adhesive fracture and 16 to 27  $\text{Jm}^{-2}$  for cohesive fracture. An extension of this approach showed that there was an apparent dependence of  $G_{Ic}$  on crack length for both alumina [37] and zirconia [38] coatings. This suggests that crack propagation is more complex in coatings than the ideal continuum model and that microstructural changes take place at the propagating crack tip region. It is unlikely that a single crack propagates through the coating, because of its lamellar structure, and complex multiple cracking is likely [39]. For simple propagation of a single crack, the critical strain energy release rate would be expected to be directly related to the true area of contact between lamellae as the crack propagates from one contact region to another. For real coatings there would be a multiplying factor, which depended on the number of multiple crack paths, having the effect of increasing the coating toughness.

### 6.3 Coating Strength

The quality of plasma sprayed coatings is often assessed by means of a tensile adhesion test such as the ASTM C633-69. Although the test is simple and provides a convenient method for comparison, its relationship to coating structure is complex. The fracture stress ( $\sigma_f$ ) for a brittle material is related, by the Griffith equation, to the size of crack like flaws ( $c$ ), the Young's modulus ( $E$ ), and the fracture surface energy ( $\gamma$ ,  $G_{Ic} = 2\gamma$ ):

$$\sigma_f = \sqrt{E\gamma/2c}$$

As discussed above,  $E$  and  $G$  are influenced by the interlamellar pores, and  $c$  will be the largest flaw present in the specimen. The variability of tensile adhesion test results would be expected to be high because of the large variations of  $c$  to be expected from sample to sample, and processing details would be expected to influence strength mainly through the effect of interlamellar contact on  $E$  and  $G_{Ic}$ .

Ault [14] noted that flame sprayed alumina coatings detached from the substrate could withstand very large strains in bending before failure and apparent strains at fracture in bending of over 1% have been reported for flame and plasma sprayed alumina [33]. Tensile tests perpendicular and parallel to the coating plane of plasma sprayed alumina coatings, however, showed negligible permanent strain at fracture [31]. The apparent „plastic“ deformation observed in bending of intrinsically brittle alumina can only arise from rearrangement of the lamellae within the coating, for example, by the opening of microcracks and fracture of some of the interlamellar contact regions. Large deformation in bending is, of course, favoured by the non-uniformity of strain about the neutral axis. The subject of coating adhesion is controversial and not well understood. The best approach would seem to be that of relating the fracture, toughness at the coating-substrate interface, which provides a measure of the resistance to failure in this region and hence “adhesion”, to microstructural details, such as fraction true contact, interface geometry and crack morphology in the vicinity of the interface [13].

### 7. THERMAL CONDUCTIVITY

Thermal conductivity is another property of plasma sprayed coatings which differs markedly from the value for the bulk material. In the case of alumina, the thermal conductivity of coatings is much less than that of sintered alumina, but increases on heat treatment at elevated temperatures [40]. It has been suggested that this is related to the fact that the coating consists of metastable alumina [41]; however, similar observations have been made for zirconia coatings suggesting that the effect is related to coating microstructure. Analysis of the thermal conductivity of coatings showed that low conductivity, in vacuum, could be satisfactorily explained because heat transfer occurred only by conduction through the regions of good contact between lamellae which were approximately 25% of the apparent area [42]. If the pores contain a gas, the conductivity increases because parallel conduction paths exist through the interlamellar pores. However, the very small width of the pores, comparable to the mean free path of the gas molecules, greatly limits conduction through these paths. Values estimated from this mode were in good agreement with experimental data. The increase in conductivity on heat treatment can thus be explained by sintering and increased interlamellar contact.

8. CONCLUSIONS

A significant feature of plasma sprayed alumina coatings is the formation of a metastable spinel type crystal structure which can be explained in terms of the nucleation kinetics of alternative crystalline forms from the melt. The detailed structure of the metastable form observed in coatings, usually referred to as  $\gamma$ - $\text{Al}_2\text{O}_3$ , differs from the  $\gamma$ - and  $\eta$ -forms of the usual nomenclature, and should, strictly, be given a new name.

The mechanical, thermal, and probably other properties, of thermally sprayed alumina coatings are dominated by their lamellar microstructure, in particular, limited interlamellar contact. The microstructure also results in anisotropic behaviour. There is some evidence that the extent of interlamellar contact is improved by low pressure spraying and the use of higher particle velocities.

References

- [1] Riley M. W., *Mater. and Methods.*, **42**, 96 (1955).
- [2] Tucker R. C., *J. Vac. Sci. Technol.*, **11**, 725 (1974).
- [3] Mash, D. R. N. E. Weare and Walker, D. L., *J. Metals.*, **13**, 473 (1961).
- [4] Steffens H., D., in „*Coatings for High Temperature Applications*“, Appl. Science, London, 1983, p. 121.
- [5] Smith M. F. and Dykhuizen R. C., *Surf. Coat. Technol.*, **34**, 25 (1988).
- [6] Henner R., Bradke M. V., Schiller G., Schumberger W. and Weber W., Proc. 12th Int. Conf. Thermal Spraying, London, 1989.
- [7] Vardelle A., Vardelle M., McPherson R. and Fauchais P., Proc. 9th. Int. Conf. Thermal Spraying, Amsterdam (1980) 155.
- [8] Chuanxian Ding, Zatorski R. A., Herman H. and Ott D., *Thin Solid Films*, **118**, 467 (1984).
- [9] Nicoll A. R., *Surf. Coat. Technol.*, **30**, 223 (1987).
- [10] Madejski J., *Int. J. Heat Mass Transferr.*, **19**, 1009 (1976).
- [11] McPherson R., *J. Mater. Sc.*, **15**, 3141 (1980).
- [12] Arata Y., Ohmori A., and Li C-J. Proc. ATTAC 88, High Temp. Soc., Japan, Osaka 05 (1988).
- [13] PePherson R., *Thin Solid Films*, **83**, 297 (1981).
- [14] Ault N. N., *J. Amer. Ceram. Soc.*, **40**, 69 (1957).
- [15] Plummer M., *J. Appl. Chem.*, **8**, 35 (1958).
- [16] McPherson R., *J. Mater. Sc.*, **8**, 851 (1973).
- [17] Hamatami H., Okada T. and Yoshida T., Proc. 9th. Int. Conf. Plasma Chem., ed. R. d'Agostino, Pugnochiuso, (1989) 1527.
- [18] Dager A., Fargeot D. and Lortholary P., *Sci. Ceram.*, **10**, 201 (1980).
- [19] Dager A., Fargeot D., Lortholary P., *Sci. Ceram.*, **11**, 157 (1981).
- [20] Boch P., Fargeot D., Gault C. and Platon F., *Rev. Int. Hautes Temper. Refract*, **18**, 85 (1981).
- [21] Lefebvre A., *J. Appl. Cryst.*, **8**, 235 (1975).
- [22] Leonard A. J., Semaille P. N. and Fripiat J. J., Proc. Brit. Ceram. Soc., **13**, 103 (1964).
- [23] Thompson V. S. and Whittemore O. J., *Bull. Amer. Ceram. Soc.*, **47**, 637 (1968).
- [24] Huffadine J. B. and Thomas A. G., *Powd. Met.*, **7**, 290 (1964).
- [25] Safai S. and Herman H., *Treat. Mater. Sc. Tech.*, **20**, 183 (1981).
- [26] Kuroda K., Hanagiri S., Suginosita M., Taira H., Tamura S., Saka H., Imura T., I. S. I. J. *Int.*, **29**, 234 (1989).
- [27] Krauth A., Meyer H., *Ber. Deutsch. Keram. Ges.*, **42**, 61 (1965).
- [28] McPherson R. and Shafer B. V., *Thin Solid Films*, **97**, 201 (1982).
- [29] Vardelle M. and Besson J. L., *Ceram. Int.*, **7**, 48 (1981).
- [30] Arata Y., Ohmori A., Li C-J., *Thin Solid Films*, **156**, 315 (1988).
- [31] McPherson R. and Cheang P., Proc. CIMTEC-7, Montecatini—Terme, (1990) (in press).
- [32] Fargeot D., Platon F. and Boch P., *Sci. Ceram.*, **9**, 382 (1977).
- [33] Shi K.-S., Qian Z.-Y. and Zhuang M.-S., *J. Amer. Ceram. Soc.*, **71**, 924 (1988).
- [34] Knudsen F. P., *J. Amer. Ceram. Soc.*, **45**, 94 (1962).
- [35] Cheang P. and McPherson R., *Thin Solid Films*, (in press).

**McPherson:**

- [36] Berndt C. C., McPherson R., *Mater. Sc. Res.*, *14*, 619 (1981).
- [37] Ostojic P. and McPherson R., *J. Amer. Ceram. Soc.*, *71*, 891 (1988).
- [38] Heintze G. N. and McPherson R., *Surface Coat Technol.*, *34*, 15 (1988).
- [39] McPherson R., *Surface Coat. Technol.*, *39/40*, 173 (1989).
- [40] Wilkis K. E. and Lagerdrost J. F., NASA Report, No. CR 121144 (1973).
- [41] Fielder H. C., *Proc. Mater. Res. Symp.*, *30*, 173 (1984).
- [42] McPherson R., *Thin Solid Films*, *112*, 89 (1984).